EPR Study of the Oxygen Evolving Complex in His-Tagged Photosystem II from the Cyanobacterium *Synechococcus elongatus*[†]

Alain Boussac,*,[‡] Miwa Sugiura,[§] Yorinao Inoue,[∥] and A. William Rutherford[‡]

Section de Bioénergétique, DBCM, URA CNRS 2096, CEA Saclay, 91191 Gif sur Yvette Cedex, France, Department of Applied Biological Chemistry, Osaka Prefecture University, 1-1 Gakuen-cho, Sakai, Osaka, 599-8531 Japan, and RIKEN Harima Institute, Spring-8 Kouto, Mikadzuki, Sayo, Hyogo 679-5148 Japan

Received May 22, 2000; Revised Manuscript Received August 24, 2000

ABSTRACT: The Mn_4-cluster and the cytochrome c_{550} in histidine-tagged photosystem II (PSII) from *Synechococcus elongatus* were studied using electron paramagnetic resonance (EPR) spectroscopy. The EPR signals associated with the S_0-state (spin = 1/2) and the S_2-state (spin = 1/2 and IR-induced spin = 5/2 state) were essentially identical to those detected in the non-His-tagged strain. The EPR signals from the S_3-state, not previously reported in cyanobacteria, were detectable both using perpendicular (at g = 10) and parallel (at g = 14) polarization EPR, and these signals are similar to those found in plant PSII. In the S_3-state, near-infrared illumination at 50 K induced a 176-G-wide split signal at g = 2 and signals at g = 5.20 and g = 1.51. These signals differ slightly from those reported in plant PSII [Ioannidis, N., and Petrouleas, V. (2000) *Biochemistry 39*, 5246−5254]. In accordance with the cited work, the split signal presumably reflects a radical interacting with the Mn_4-cluster in a fraction of centers, while the g = 5.20 and g = 1.51 signals are tentatively attributed to a high-spin state of the Mn_4-cluster with zero field splitting parameters different from those in plant PSII, reflecting minor changes in the environment of the Mn_4-cluster. Biochemical modifications (Sr^{2+}/Ca^{2+} substitution, acetate and NH_3 treatments) were also investigated. In Sr^{2+}-reconstituted PSII, in addition to the expected modified S_2 multiline signal, a signal at g = 5.2 was present instead of the $g \approx 4$ signal seen in plant PSII. In NH_3-treated samples, in addition to the expected modified S_2-multiline signal, a $g \approx 4$ signal was detected in a small proportion of the reaction centers. This is of note since $g \approx 4$ spectra arising from the Mn_4-cluster in the S_2 state have not yet been published in cyanobacterial PSII. The detection of modified S_3-signals in both perpendicular (at g = 7.5) and parallel (at g = 12) polarization EPR from NH_3-treated PSII indicate that NH_3 is still bound in the S_3-state. The acetate-treated PSII behaves essentially as in plant PSII. A study using oriented samples indicated that the heme plane of the oxidized low spin Cytc_{550} was perpendicular to the plane of the membrane.

The evolution of oxygen as a result of light-driven water oxidation is catalyzed by photosystem II (PSII)[1] in which a cluster of four manganese ions acts both as a device for accumulating oxidizing equivalents and as the active site. The reaction center of PSII is made up of two membrane-spanning polypeptides (D1 and D2) analogous to the L and M subunits of the purple photosynthetic bacterial reaction center (*1*, *2*). Absorption of a photon results in a charge separation between a chlorophyll molecule (P_{680}), and a pheophytin molecule. The pheophytin anion transfers the electron to a quinone, Q_A, and $P_{680}{}^+$ is reduced by a tyrosine residue, Tyr_Z, which in turn is reduced by the Mn_4-cluster. During the enzyme cycle, the oxidizing side of PSII goes through five different redox states that are denoted S_n, n varying from 0 to 4. Oxygen is released during the S_3 to S_0 transition in which S_4 is a transient state (*3*−*7*).

The structure of the Mn_4 cluster and the mechanism by which water is oxidized are still largely unknown. Currently, the most commonly discussed structure, mainly based on EXAFS data and to some extent EPR data, consists of a Mn tetramer that includes two di-μ-oxo(Mn_2) motifs (reviewed in ref *7*). As for valence, the majority view is that the S_1-state consists of two Mn^{III} and two Mn^{IV} ions and that the S_0 to S_1 and the S_1 to S_2 steps each corresponds to one-electron oxidation of the Mn cluster. For the S_2 to S_3 transition, several lines of evidence have led to the suggestion that a ligand-centered oxidation may occur rather than the conventional view of metal-centered oxidation (ref *8* and references therein).

EPR has played an important role in studying the oxygen evolving complex. EPR signals from the S_0-, S_1-, S_2- and

[†]This work was in part supported by a grant from the TMR program of the EC (FMRX-CT98-0214).

* To whom correspondence should be addressed. Tel: 33 1 68 08 72 06. Fax: 33 1 69 08 87 17. E-mail: boussac@dsvidf.cea.fr.

[‡] URA CNRS 2096.

[§] Prefecture University.

[∥] RIKEN Harima Institute.

[1] Abbreviations: P_{680}, photooxidisable chlorophyll (Chl) of photosystem II (PSII); Tyr_Z, the tyrosine acting as the electron donor to P_{680}; Tyr_D, the tyrosine acting as a side path electron donor to P_{680}; Q_A and Q_B, primary and secondary quinone electron acceptor of PSII; EPR, electron paramagnetic resonance; PPBQ, phenyl-*p*-benzoquinone; DMSO, dimethyl sulfoxide; MES, 2-(*N*-morpholino) ethanesulfonic acid; HEPES, *N*-2-hydroxyethylpiperazine-*N*′-2-ethanesulfonic acid; EGTA, ethylene glycol bis(β-aminoethyl ether)-*N*,*N*,*N*′,*N*′ tetraacetic acid; EDTA, ethylene-diamine-tetraacetate.

10.1021/bi001159r CCC: $19.00
Published on Web 10/13/2000

S_3-states have now been detected in PSII. While the signals from S_2 have been known for some time, the signals from the other states have been reported only relatively recently. In the following, we shall briefly review the EPR literature on these states.

The S_2-State. The Mn-cluster gives rise to several EPR signals in the S_2-state: a so-called multiline signal (*9*) and signals from at least two different high-spin (ground) states.

The multiline signal is centered around $g = 2$ and is spread over roughly 1800 G, is made up of at least 18 lines, each separated by approximately 80 G, and arises from a spin 1/2 (ground) state, very probably from a magnetic Mn-tetramer, $Mn^{III}{}_3Mn^{IV}$ or $Mn^{IV}{}_3Mn^{III}$ (ref *10* and references therein). Several modified forms of the S_2-multiline signal have been observed depending on biochemical treatments of the enzyme (*11*−*13*). The cases relevant to the present study are the following: (i) In the ammonia-treated enzyme (*11*), the S_2-multiline signal exhibits 21−22 hyperfine lines with reduced hyperfine spacing. This modifications was interpreted as arising from the formation of an amido(NH_2) bridge in the $Mn^{III}Mn^{IV}$ dimer of the Mn_4-cluster (*14*). (ii) When Sr^{2+} is substituted for Ca^{2+} in the O_2-evolving enzyme, another modified S_2-multiline signal is observed (*12*). This signal is similar, but not identical, to that observed in NH_3-treated PSII.

The better known high-spin state from S_2 is that giving rise to a signal around $g \approx 4$ and such signals are seen under two different classes of experimental conditions (*15*−*20*). First, the $g \approx 4$ signal can be generated by illumination at room temperature or at 200 K. The fraction of centers giving rise to this $g \approx 4$ signal is dependent on the pretreatment of the enzyme, being markedly increased by (i) having sucrose present in the medium (*15*, *16*), (ii) certain treatments that remove chloride from the medium (*21*, *22*) or its replacement by F^- (*17*, *23*), I^- (*23*, *24*), amines (*25*), or NO_3^- (*23*), and (iii) replacing Ca^{2+} with Sr^{2+} (*12*). Second, the $g \approx 4$ signal can also be generated by near-infrared illumination of the S_2-multiline state, between 77 and 170 K. This represents a IR-induced spin-state transition in the Mn_4 cluster, from spin 1/2 to spin 5/2 (*19*, *20*, *26*). Above 170 K, the infrared-induced spin 5/2 S_2-state converts back into the spin 1/2 S_2-multiline state. The $g = 4.1$ signals produced under the different conditions described above arise from similar spin 5/2 states (*19*, *20*, *26*, *27*) but which have quite different stability in terms of temperature (*20*).

A third type of signal from the S_2 state was reported. Signals at g values > 5 were found when the spin 1/2 state was illuminated with IR light below 77 K. Between 77 and 170 K, a relaxation process occurs leading to formation of the $g = 4$ signal. The new $g > 5$ signals were attributed to a high-spin state (probably a spin = 5/2) representing a state of the Mn_4-cluster similar to that giving rise to the $g = 4$ signal but in a slightly different (unrelaxed) environment (*28*, *29*).

For the S_2-state, some spectroscopic differences between plant PSII and PSII from *S. elongatus* have been found (*29*, *30*). Methanol has no effect on the hyperfine structure of the S_2-multiline signal in *S. elongatus*, and it does not inhibit the infrared-induced spin-state transition in contrast with the situation in plant PSII. Moreover, the value of the zero field splitting parameters (E/D and D) found for the infrared-induced $g > 5$, spin 5/2 state in PSII isolated from *S. elongatus* corresponded to a more rhombic structure than those found for the spin 5/2 state in PSII from spinach. Furthermore, the relative stability of these states versus the $g = 4$ state differs between plants and cyanobacteria, indeed the absence of $g = 4$ signal in PSII from *S. elongatus* has been attributed to the increased stability of the $g > 5$ state which decays directly to the spin = 1/2 state without giving rise to a detectable $g = 4$ intermediate. All of these effects have been interpreted as being the consequences of small differences in the ligand environment of the Mn_4-cluster.

The S_0-State. S_0 also gives rise to a multiline EPR signal centered near $g = 2$ (*31*−*34*). It is spread over ≈ 2380 G and is constituted of 25 resolved lines spaced by 65−95 G. It originates from the Mn_4-cluster in a spin 1/2 ground state and is tentatively attributed to a $Mn^{IV}{}_2{-}Mn^{III}Mn^{II}$ or $Mn^{III}{}_2{-}Mn^{III}Mn^{II}$ complex. The S_0-multiline signal has been observed in plant PSII in the presence of methanol (*31*−*34*) and in PSII cores from *S. elongatus* (*30*). Although it was shown that alcohols are not required to observe the S_0-signal in *S. elongatus* (*30*), addition of methanol increased its resolution. The S_0-multiline signals detected in plant PSII and in *S. elongatus* were similar but not identical.

The S_1-State. The use of parallel polarization EPR spectroscopy allowed the detection of signals in the S_1-state. Two signals have been reported: (i) a broad featureless signal at $g = 4.8$ (*35*, *36*) and (ii) a multiline signal centered at $g = 12$ with at least 18 lines spaced by 32 G (*37*, *38*). The S_1-multiline signal was observed in PSII core preparations from *Synechocystis* and in plant PSII in which the 17- and 23-kDa extrinsic proteins had been removed.

The S_3-State. EPR signals in the S_3-state have been detected in plant PSII using both perpendicular (at $g = 6.7$) and parallel (at $g = 12$ and $g = 8$) polarization modes (*39*, *40*). These signals were interpreted as originating from different transitions in the same spin = 1 state (*39*). Interestingly, it was found that, in the S_3-state, near-infrared light induced new EPR signals in a fraction of the reaction centers (*40*).

This brief review covers a small fraction of the papers on the S_2 state but nearly all of the articles on the EPR of the other S states. The relative paucity of reports on the EPR signals arising from S states other than S_2 reflects not only their more recent discovery but also the fact that they are in general more difficult to detect and that special conditions or nonconventional EPR methods are required. The use of these new signals to obtain structural and mechanistic information requires improved biological samples, having a higher purity and yet maintaining the homogeneity characteristic of the less purified samples used for the majority of studies up to now (i.e., PSII-enriched membranes).

One such biological preparation is the so-called "PSII core" preparation from the thermopilic cyanobacterium, *S. elongatus*. PSII in this species is more stable than that either from plants or from mesophillic cyanobacteria, and it has thus become a material widely used in attempts to generate crystals (e.g., *41*−*43*) for structural investigations. As these studies progress toward providing a detailed structural model, it seems timely to study this specific material using EPR to relate it to the extensive EPR literature obtained on plant PSII. Some EPR studies on this species have been reported; these however have focused mainly on the signals from the S_2 state and more recently from the S_0 state (see above).

The addition of a histidine extension (His-tag) to a protein of the PSII reaction center has facilitated the purification of PSII cores from *Chlamydomonas reinhardtii* (*44*), from *Synechocystis* 6803 (*45*−*47*) and from *S. elongatus* (*48*). So-called "His-tagged PSII cores" have undergone little characterisation by EPR. In the case of *Synechocystis* 6803, it was reported that the S_2 state showed an EPR signal at $g = 4$ (*45*). This was somewhat surprising since no such signal had been reported previously in cyanobacterial PSII. It thus seemed possible that the presence of the His-tag itself may modify the environment of the Mn_4-cluster.

In the present work, we have undertaken an EPR study of the S_0-, S_1-, S_2- and S_3-states in a His-tagged strain of *S. elongatus*. The study indicates that the His-tag itself does not influence the EPR of the Mn. Furthermore, this material allows the detection of signals previously unreported in cyanobacteria. Several biochemically modified forms of the enzyme have also been studied. Similarities and differences between plants and *S. elongatus* are emphasized. In addition, the cyanobacterial system contains a membrane-bound cytochrome, Cytc_{550}, that is specifically associated with the electron donor side of PSII (*49*−*53*). This cytochrome is studied by EPR, and the orientation of the heme plane relative to the membrane is determined.

MATERIALS AND METHODS

PSII cores from His-tagged CP43 *S. elongatus* were isolated as previously described (*48*). PSII samples were frozen and stored at 77 K (or in dry ice at 198 K) in a medium containing 40 mM Mes (pH 6.5), 20 mM NaCl, 15 mM $CaCl_2$, 15 mM $MgCl_2$, and 25% glycerol at a concentration of 1.3−1.5 mg of Chl/mL.

Detection of the S_2- and S_0-Multiline Signals. PSII cores were loaded into EPR tubes in the medium described above at ≈ 0.8−0.9 mg of Chl/mL. After dark adaptation for 1 h at 0 °C, the reaction centers were synchronized in the S_1-state by illuminating the samples with one flash given at room temperature (*30*). Then, after 12-min dark adaptation at room temperature, PPBQ (0.5 mM) dissolved in methanol (3 % final concentration) was added as an electron acceptor. The samples were then submitted to 0, 1, or 3 flashes and frozen immediately at 198 K in a CO_2−ethanol bath and then cooled to 77 K in liquid nitrogen.

Detection of the S_3 Signals in Untreated PSII. PSII cores were diluted (about 50 times) in a medium containing 0.3 M sucrose, 10 mM NaCl, and 25 mM Mes (pH 6.5) and then collected by centrifugation (≈ 1 h, ≈ 180000*g*) and resuspended in the same medium at about 0.8 mg of Chl/mL. Synchronization in the S_1-state and the flash sequence were done as described above except that ferricyanide (dissolved in water at 50 μM final concentration) was used as an electron acceptor instead of PPBQ.

Ammonia Treatment. PSII cores were diluted (about 50 times) in a medium containing 0.3 M sucrose, 10 mM NaCl, and 5 mM Mes (pH 6.5), and then pelleted by centrifugation and resuspended in the same medium at about 0.8 mg of Chl/mL. After dark adaptation for 1 h on ice, Hepes (pH 7.5) and NH_4Cl were added (both 100 mM, final concentration). Then, PPBQ (0.5 mM) dissolved in DMSO (3% final concentration) was added. Formation of the S_2-state was achieved by illumination at 198 K in a CO_2−ethanol bath through water and infrared filters.

Sr^{2+} Reconstitution. PSII cores were diluted (about 50 times) in a medium containing 1 M $SrCl_2$ and 25 mM Mes (pH 6.5) and incubated at 0 °C for 30 min in darkness. The PSII cores were collected by centrifugation and resuspended in a medium containing 0.3 M sucrose, 10 mM NaCl, and 25 mM Mes (pH 6.5) and 5 mM $SrCl_2$ at about 0.8 mg of Chl/mL. After dark adaptation for 1 h on ice, ferricyanide (50 μM) dissolved in water was added. Formation of the S_2-state was achieved by illumination at 198 K in a CO_2−ethanol bath through water and infrared filters.

Acetate Treatment. PSII cores were diluted (about 50 times) in a medium containing 0.5 M acetate, 40 mM Mes, 0.3 M sucrose, and 5 mM $Ca(OH)_2$ (the pH was adjusted to 5.25 with NaOH) and incubated for 30 min in darkness. The PSII cores were collected by centrifugation and resuspended in the same medium. After dark adaptation for 1 h on ice, PPBQ (0.5 mM) dissolved in DMSO (3% final concentration) was added. Then, the sample was illuminated, either at 198 K in a CO_2−ethanol bath or at 0 °C in ethanol cooled with liquid nitrogen, through water and infrared filters.

Purification of the 33-kDa Protein. The 33-kDa protein from spinach was extracted with the following protocol. PSII membranes purified as previously described were first washed with 1.2 M NaCl to remove the 17- and 24-kDa protein and then pelleted by centrifugation. The membranes were then washed in a medium containing 1 M $CaCl_2$ to remove the 33-kDa protein (*54*). After a second centrifugation the supernatant, containing the 33-kDa protein, was first dialyzed against a medium containing 25 mM Mes, pH 6.5, and 10 mM NaCl, and then concentrated. The presence of the 33-kDa was verified by SDS−PAGE (not shown).

Purification of the Cytc_{550}. Purification of the Cytc_{550} was done with the following protocol. His-tagged PSII cores from *S. elongatus* were washed with $CaCl_2$ as previously described (*48*). From SDS−PAGE analysis, almost all the Cytc_{550} seems to be removed by this protocol (*48*). After a centrifugation, the supernatant containing the Cytc_{550}, the 33-kDa and a 12-kDa protein was dialyzed against a medium containing 10 mM NaCl and 25 mM Hepes, pH 7.5. The Cytc_{550} was then purified by HPLC by using a mono QHR 5/5 column (Pharmacia). The presence of the Cytc_{550} was verified by SDS−PAGE (not shown).

Oriented Samples. Orientation of PSII cores on Mylar sheet was done essentially as previously described (*55*). PSII cores from His-tagged *S. elongatus*, after thawing, were first diluted about 50 times in a medium containing 0.03 M sucrose, 1 mM NaCl, and 2.5 mM Mes (pH 6.5), and then collected by centrifugation and resuspended in the same medium at about 1 mg of Chl/mL. Then, the resuspension was painted onto Mylar sheets and incubated for 36 h in total darkness at 4 °C in a ≈ 90% humidity atmosphere.

Flash illumination at room temperature was provided by a Nd:YAG laser (532 nm, 550 mJ, 8 ns) Spectra Physics GCR-230-10. Near-IR illumination of the samples was done in a nitrogen gas flow system (Bruker, B-VT-3000) or directly in the EPR cavity and was provided by a laser diode emitting at 820 nm (Coherent, diode S-81-1000C) with a power of 600−700 mW at the level of the sample. CW-EPR spectra were recorded using a standard ER 4102 (Bruker) or a ER 4116 DM dual mode (Bruker) X-band resonators at liquid helium temperatures with a Bruker ESP300 X-band spectrometer equipped with an Oxford

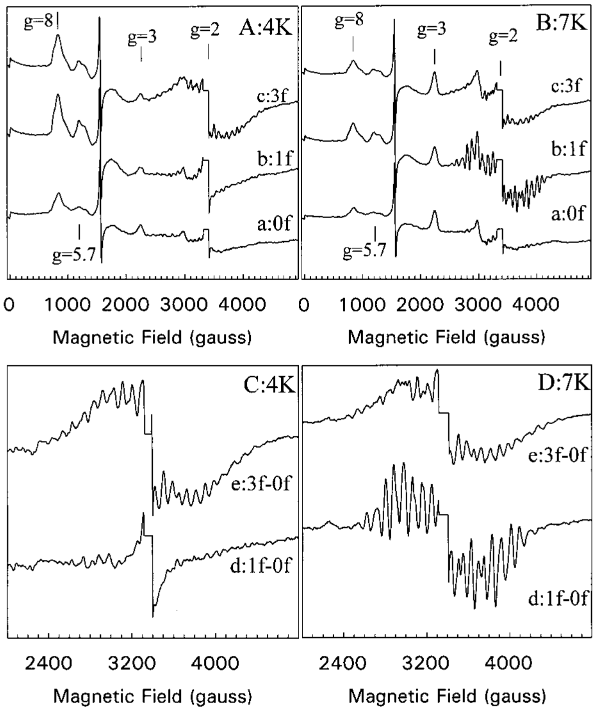

FIGURE 1: The S_2- and S_0-multiline signals. CW-EPR spectra recorded on His-tagged PSII cores isolated from *S. elongatus* after a series of saturating laser flashes (1 Hz) in the presence of methanol. Spectra in panels A and C and panels B and D were recorded at 4 and 7 K, respectively. Spectra in panels C and D correspond to the light-minus-dark spectra shown in panels A and B, respectively. Other instrument settings: standard cavity; modulation amplitude, 25 G; microwave power, 20 mW; microwave frequency, 9.4 GHz; modulation frequency, 100 kHz. The central part of the spectra corresponding to the Tyr_D region was deleted.

Instruments cryostat (ESR 900 or ESR 910). Before the recording of all spectra, samples were degassed as previously described (*28*).

RESULTS

The S_2- and S_0-Multiline Signals. Figure 1 shows the CW-EPR spectra recorded at 4 K (panel A) or 7 K (panel B) on PSII cores isolated from His-tagged *S. elongatus*. Spectra a in panels A and B of Figure 1 were recorded in dark-adapted PSII (i.e., in the S_1-state), and spectra b were recorded after one flash (i.e., in the S_2-state). After the third flash (spectra c), the S_0-state is the predominant S-state, and therefore the multiline signal recorded in these conditions mainly originates from the S_0-state. The S_0-multiline signal is favored at 4 K while the S_2-multiline signal, in these samples containing methanol, is favored at 7 K (*30*, *34*). Under the microwave power used here (20 mW), the S_2-multiline signal is not detectable at 4 K.

Figure 1, panels C and D, shows the light-minus-dark spectra recorded at 4 K or at 7 K, respectively. The S_2-multiline signal (spectrum d, panel D) and the S_0-multiline signal (spectra e, panels C and D) are essentially identical to those previously detected in non His-tagged *S. elongatus* (*30*).

In spectra a, b, and c the following features are also present: (i) signals at ≈ 2230 G and ≈ 3030 G, particularly evident at 7 K, attributed to the g_z and g_y resonances, respectively, of oxidized low-spin cytochrome heme(s). These features are much more intense in *S. elongatus* than in plant PSII. As proposed previously (*29*, *30*), it seems likely that the increase in these signals arises from the presence of the Cytc_{550} signal (see below), which is expected to be oxidized plus any fraction of centers that may have Cytb_{559} in its oxidized form; (ii) signal at ≈ 1600 G from contaminant high-spin Fe^{3+}; (iii) signals at 850 G (i.e., $g = 8$) and 1200 G (i.e., $g = 5.7$) from the oxidized non-heme iron $Q_AFe^{3+}Q_B$.

The presence of $Q_AFe^{3+}Q_B$ is explained as follows: after dark adaptation, the $Q_AFe^{2+}Q_B^-$ state is present in a fraction of the PSII cores. This was seen by the presence of the $g = 1.6$ signal (arising from the $Q_A^-Fe^{2+}Q_B^-$ state) when low-temperature illumination was given to a dark-adapted sample (not shown). Addition of PPBQ resulted in formation of the $Q_AFe^{3+}Q_B$ state in these centers due to oxidation of iron by $PPBQ^-$. Then, illumination by one flash resulted in the formation of the $Q_AFe^{2+}Q_B$ state, while the $Q_A^-Fe^{2+}Q_B$ state and then the $Q_AFe^{3+}Q_B$ state were formed in the other reaction centers (*56*). From the amplitude of the $g = 8$ and $g = 5.7$ signals in spectra a, b, and c in panel A of Figure 1, it can be roughly estimated that, after dark-adaptation, the $Q_AFe^{2+}Q_B^-$ state was present in about 30% of the reaction centers.

The S_1-state. We looked for the S_1-multiline signal in PSII cores from untreated-His-tagged PSII from *S. elongatus* by using parallel polarization EPR but were unable to find conditions under which a signal could be detected. In *Synechocystis* 6803, the species in which this signal was discovered (*37*, *38*), the Cytc_{550} is not bound to the PSII cores in contrast with the situation in *S. elongatus*. Thus we looked for the S_1-multiline signal after the removal of Cytc_{550} in *S. elongatus* by a $CaCl_2$ washing of PSII cores but with no success. Since the $CaCl_2$ washing also removes the 33-kDa protein and since, in plant PSII, it has been shown that the presence of this protein was required to detect the S_1-multiline (*38*), we looked for the S_1-signal after the addition of a 10-fold excess of the 33-kDa protein isolated from spinach (*57*) but again with no success. It is worthy of note that we were able to detect the S_1 multiline signal in salt-washed PSII from plants (not shown). We conclude therefore that the inability to detect the signal in *S. elongatus* is more likely to be attributable to the fact that we have not yet obtained the appropriate biochemical conditions. It is perhaps of further note that we have not been able to detect the broader parallel mode EPR signal attributed to S_1 (*35*) in any of our studies.

The S_3-State. Figure 2 shows an experiment in which the S_3-signals were looked for in His-tagged PSII from *S. elongatus*. It has been previously shown that the addition of organic solvents makes the S_3-state more or less undetectable (*39*, *40*). For that reason, for these experiments, potassium ferricyanide (dissolved in water) was used as an electron acceptor. In Figure 2, spectra a, b, and c in panel A were recorded after 0, 1, and 2 flashes, respectively, using perpendicular mode EPR. Spectrum b exhibits a strong S_2-mutiline signal. After two flashes (spectrum c), the amplitude of the S_2-multiline is 24% of that measured after the first flash. This indicates efficient S-state turnovers with an initial population of S_1 greater than 95% and misses lower than 10%. The fraction of centers in the S_3-state after 2 flashes can be estimated to ≈ 75%. These data indicate that the low concentration of ferricyanide used (i.e., 50 μM) was not

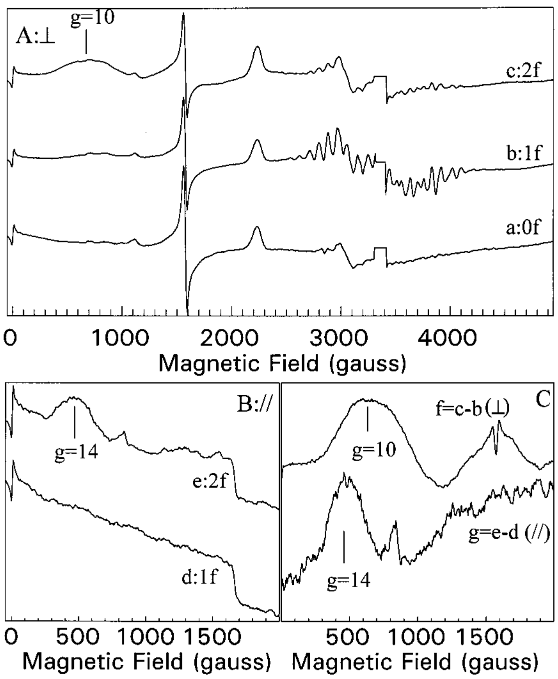

FIGURE 2: The S_3-signals. CW-EPR spectra recorded on His-tagged PSII cores isolated from *S. elongatus* after a series of saturating laser flashes (1 Hz). Spectra in panels A and B were recorded by using a perpendicular or parallel polarization mode, respectively. Other instrument settings for panel A: standard cavity; temperature, 8 K; modulation amplitude, 25 G; microwave power, 20 mW; microwave frequency, 9.4 GHz; modulation frequency, 100 kHz. The central part of the spectra corresponding to the Tyr_D region was deleted. Other instrument settings for panel B: dual mode cavity; temperature, 4.2 K; modulation amplitude, 12.5 G; microwave power, 20 mW; microwave frequency, 9.34 GHz; modulation frequency, 100 kHz. Spectra in panel C correspond to the light-minus-dark spectra shown in panels A and B.

limiting, at least for illumination by two flashes. This is not surprising because, in *S. elongatus*, the secondary quinone, Q_B, is present and able to efficiently oxidize Q_A^- (*48*) (see also above).

After two flashes (Figure 2, spectrum c, panel A), a signal centered at $g = 10$ is detected by parallel polarization EPR. This signal is very similar to that detected in the S_3-state in plant PSII (*39*, *40*).

Spectra d and e in panel B of Figure 2 were recorded after 1 and 2 flashes, respectively, using parallel mode EPR. No signal was observed after one flash, while after two flashes a signal centered at $g = 14$ is present. This signal bears also strong resemblance to the S_3-signal previously detected in plant PS II (*39*, *40*). Figure 2, panel C shows the 2 flashes-minus-1 flash spectra using perpendicular (spectrum f) or parallel (spectrum g) polarization EPR. Decreasing the temperature to 1.8 K improved the detection of the S_3-signals both with parallel and perpendicular polarization (not shown).

The S_2-State in Ammonia-Treated PSII. In Figure 3, the effects of ammonia (spectra a and b) were investigated in His-tagged PSII cores from *S. elongatus*. Spectrum a corresponds to the light-minus-dark spectrum induced by illumination at 190 K of PSII cores incubated at pH 7.5 in the presence of ammonia. Illumination at 190 K resulted in the formation of a normal S_2-multiline signal as observed in plant PSII (*11*, *25*, *58*). Spectrum a also exhibits negative signals at $g = 8$ and $g = 5.7$. This shows that the oxidized form $Q_AFe^{3+}Q_B$ was present in a proportion of the dark-

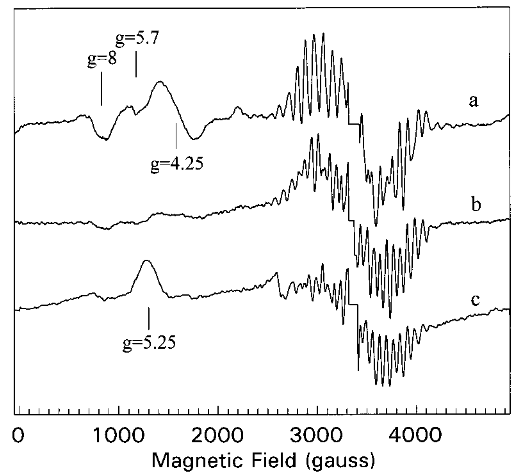

FIGURE 3: Effect of ammonia and Sr^{2+} in S_2. Spectrum a: light-minus-dark spectrum recorded after illumination at 190 K of ammonia-treated His-tagged PSII cores from *S. elongatus*. Spectrum b: light-minus-dark spectrum recorded after the warming up to 250 K, in the dark, of the 190 K illuminated ammonia-treated His-tagged PSII from *S. elongatus*. Spectrum c: light-minus-dark spectrum recorded after illumination at 198 K of a Sr^{2+}-reconstituted His-tagged PSII cores from *S. elongatus*. Instrument settings: standard cavity; temperature, 8 K; modulation amplitude, 25 G; microwave power, 20 mW; microwave frequency, 9.4 GHz; modulation frequency, 100 kHz. The central part of the spectra corresponding to the Tyr_D region was deleted.

adapted PSII cores. Finally, spectrum a shows that a signal at $g = 4.25$ is also induced by the illumination at 190 K. Such a signal at $g = 4.25$ has been observed in ammonia-treated plant PSII (*11*, *25*, *58*) and has been attributed to centers in which ammonia competes with Cl^- (*25*, *59*) in the S_1-state. We attribute the $g = 4.25$ signal seen here in *S. elongatus* to a spin 5/2 S_2-state, as in plant PSII.

After illumination at 190 K, the sample was warmed in the dark to 250 K for $\approx$ 10 s. Then, the sample was rapidly cooled to 77 K and the EPR spectrum was recorded at 8 K. Spectrum b in Figure 3 corresponds to the spectrum recorded after the warming of the sample minus that recorded before illumination at 190 K. Spectrum b exhibits a modified S_2-multiline signal essentially identical to that observed in ammonia-treated plant PSII (*11*, *25*, *58*). The quality of this spectrum is higher than that measured in ammonia-treated PSII from *Synechocystis* (*60*).

The $g = 4.25$ signal is no longer detected in spectrum b. As observed in ammonia-treated PSII from spinach (see ref *58* and references therein) warming to 250 K may allow the $g = 4$ state to convert into the S_2-multiline state.

It is of note that the negative signals at $g = 8$ and $g = 5.7$ are greatly diminished in the difference spectrum (spectrum b) upon warming to 250 K. This may be easily explained if we assume that, before the 190 K illumination, the $Q_AFe^{3+}Q_B$ state was present in about 50% of the ammonia-treated PSII cores (see above), while the $Q_AFe^{2+}Q_B$ state was present in the other 50%. If so, illumination at 190 K resulted in the formation of the $Q_AFe^{2+}Q_B$ state in the first 50% and in the formation of the $Q_A^-Fe^{2+}Q_B$ state in the other 50%. Then, upon warming to 250 K and in the presence of PPBQ (see above), the $Q_A^-Fe^{2+}Q_B$ state converted into the $Q_AFe^{3+}Q_B$ state. In this model, reduction of the non-heme iron occurred in 50% of the PSII cores and oxidation of the non-heme iron occurred in the other 50%.

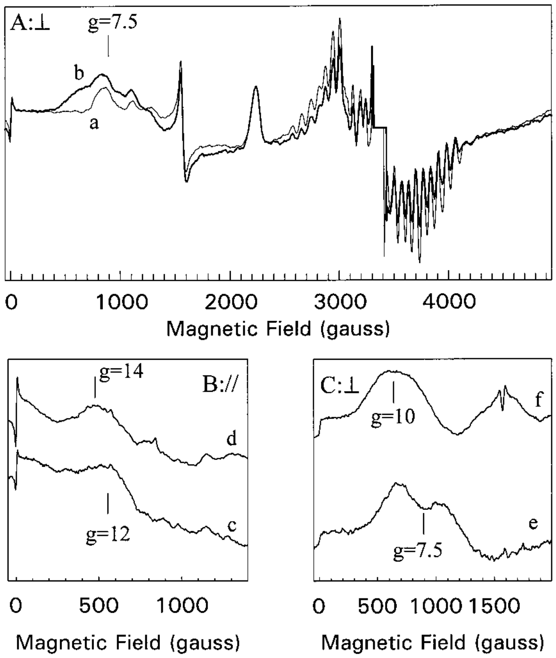

FIGURE 4: Effect of ammonia in S_3. CW-EPR spectra recorded on ammonia-treated His-tagged PSII cores isolated from *S. elongatus*. Spectra in panel A and spectra in panel B were recorded by using a perpendicular or parallel polarization mode, respectively. Spectrum a was recorded after illumination at 190 K. Spectra b and c were recorded after a further illumination by one laser flash at room temperature. Spectrum d in panel B is a re-plot of spectrum e in Figure 2, panel B. In panel C, spectrum e corresponds to spectrum b minus spectrum a in panel A, and spectrum c is a re-plot of spectrum f in Figure 2, panel C. Other instrument settings for panel A: standard cavity; temperature, 8 K; modulation amplitude, 25 G; microwave power, 20 mW; microwave frequency, 9.4 GHz; modulation frequency, 100 kHz. The central part of the spectra corresponding to the Tyr_D region was deleted. Other instrument settings for panel B: dual mode cavity; temperature, 4.2 K; modulation amplitude, 12.5 G; microwave power, 20 mW; microwave frequency, 9.34 GHz; modulation frequency, 100 kHz.

The S_2-State in Sr^{2+}-Reconstituted PSII. Spectrum c in Figure 3 corresponds to the light-minus-dark spectrum induced by illumination at 198 K of Sr^{2+}-reconstituted PSII cores from His-tagged *S. elongatus*. The amplitude of this spectrum has been arbitrarily scaled to that of spectra a and b. The Ca^{2+} substitution for Sr^{2+} resulted in a modified S_2-multiline signal similar to that observed in plant PSII (*12*) and in *Synechocystis* (*60*). Although the Sr^{2+}-reconsituted plant PSII exhibits a strong $g = 4.25$ signal in the absence of alcohol, here no $g \approx 4$ signal was observed in *S. elongatus*. Instead, a signal with a maximum at $g = 5.25$ was observed.

The S_3-State in Ammonia-Treated PSII. After the recording of spectrum b in Figure 3 (replotted without a background subtraction as spectrum a in panel A of Figure 4), the ammonia-treated sample was rapidly thawed in the dark (this operation took 5−10 s) and immediately illuminated by a laser flash at room temperature. Then, the sample was frozen immediately at 198 K then to 77 K before recording the EPR spectra by using perpendicular (spectrum b in panel A) and parallel (spectrum c in panel B) polarization EPR.

In this experiment, no synchronization of the PSII cores in the S_1-state was done, i.e., we assume that about 75% of the centers are in the S_1-state prior to the 198 K illumination. Since the amplitude of the modified S_2-multiline signal after the laser flash (spectrum b in panel A) is about 55% of that before the laser flash (spectrum a in panel A), it can be roughly estimated that the S_3-state has been formed in ≈ 50% of the PSII cores.

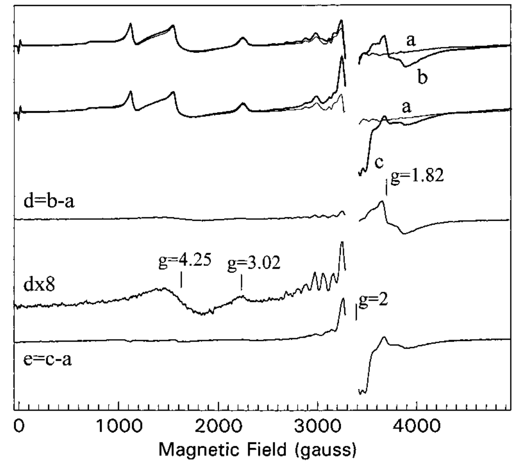

FIGURE 5: Effect of acetate. CW-EPR spectra recorded on acetate-treated His-tagged PSII cores isolated from *S. elongatus*. Spectrum a was recorded on a dark-adapted sample. Spectrum b was recorded after illumination at 198 K. Spectrum c was recorded after illumination at 0 °C. Other instrument settings: standard cavity; temperature, 8 K; modulation amplitude, 25 G; microwave power, 20 mW; microwave frequency, 9.4 GHz; modulation frequency, 100 kHz. The central part of the spectra corresponding to the Tyr_D region was deleted.

Although the S_3 population was not maximal, a new signal centered at $g = 7.5$ is present in spectrum b. Spectrum e in panel C of Figure 4 corresponds to the difference spectrum resulting from spectrum b-minus-spectrum a in panel A and is compared to the S_3-signal in untreated PSII (spectrum f). Although spectrum e could be slightly contaminated by signals from the non-heme iron (due to changes in the proportion of oxidized iron), the center of the S_3-signal in ammonia-treated PSII appears shifted from $g = 10$ to $g = 7.5$ when compared to that observed in untreated PSII.

With the parallel mode detection (panel B), the spectrum recorded in the S_3-state of ammonia-treated PSII (spectrum c) appeared also slightly shifted from $g = 14$ to $g = 12$ when compared to the signal recorded in the untreated S_3-state (spectrum d).

Acetate-Treated PSII. In Figure 5, effects of acetate-treatment on His-tagged PSII cores from *S. elongatus* were investigated by EPR at low temperature. Spectrum a in Figure 5 was recorded on a dark-adapted sample and spectrum b was recorded after illumination at 198 K. Spectrum d corresponds to the light-induced spectrum at 198 K. It exhibits mainly a strong $Q_A^-Fe^{2+}Q_B$ signal at $g = 1.82$ as observed in acetate-treated PSII (*61*, *62*). This indicates that in *S. elongatus*, acetate is able to bind to the non-heme iron, as originally reported for formate in plant PSII (*63*). Magnification of spectrum d shows that a small S_2-multiline signal and a small signal at $g = 4.25$ were induced by the illumination at 198 K. The signal at $g = 3.02$ is very probably due to the oxidation of Cytb_{559} in a small proportion of the PSII cores.

Spectrum c in Figure 5 was recorded after illumination at 0 °C followed by rapid freezing at 198 K then at 77 K. The light-induced spectrum at 0 °C (spectrum e) exhibits a split

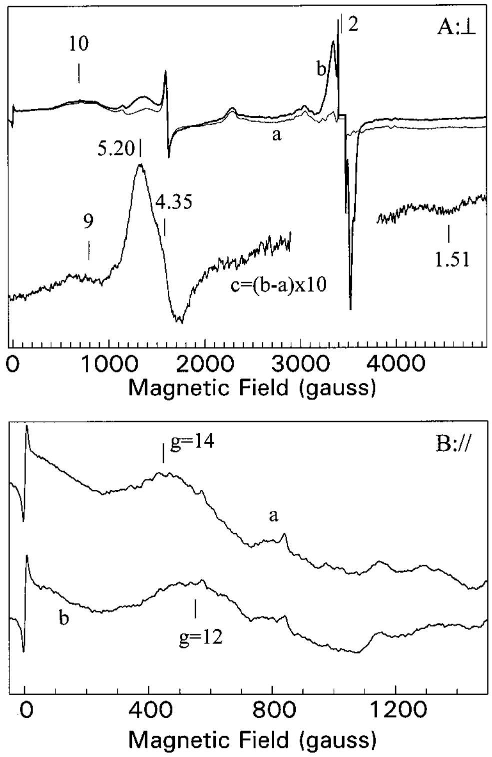

FIGURE 6: Effect of near-infrared light in S_3. Spectra in panels A and B were recorded by using a perpendicular or parallel polarization mode, respectively. Spectra a were recorded after two flashes (same protocol as in Figure 2). Spectra b were recorded after an additional illumination at 820 nm at 50 K in the EPR cavity for 2 min. Other instrument settings for panel A: dual mode cavity; temperature, 4.2 K; modulation amplitude, 12.5 G; microwave power, 20 mW; microwave frequency, 9.34 GHz; modulation frequency, 100 kHz. The central part of the spectra corresponding to the Tyr_D region was deleted. Other instrument settings for panel B: dual mode cavity; temperature, 4.2 K; modulation amplitude, 12.5 G; microwave power, 20 mW; microwave frequency, 9.34 GHz; modulation frequency, 100 kHz.

signal with a width of 232 G (peak to trough). Despite the presence of PPBQ, a small proportion of $Q_A^-Fe^{2+}Q_B$ is detected at $g = 1.82$ in spectrum c.

The acetate-induced split signal observed in PSII from *Synechocystis* (*64*) has been attributed to $S_2Tyr_Z^\bullet$. Therefore, the similar 232-G wide, split signal observed here is also attributed to $S_2Tyr_Z^\bullet$. The small signal at $g = 4.25$ and the residual multiline signal may be attributable to a small fraction of the centers where the acetate effect is incomplete. In plant PSII treated with acetate, upon laser flash illumination of dark-adapted membranes (i.e., PSII in the S_1-state), the proportion of centers in which the $S_2Tyr_Z^\bullet$ signal was formed on the second flash was considerably lower than the proportion of centers in which the S_2-multiline and $g = 4.25$ signals disappeared (Boussac, unpublished observations). The simplest explanation for this result is that the $g = 4.1$ signal and the S_2 multiline signal detected after illumination at 198 K arose from centers different from those in which the split $S_2Tyr_Z^\bullet$ signal was observed upon 0 °C illumination. This may be due to a partial effect of acetate, i.e., a partial chloride-depletion in a low proportion of the reaction centers.

Near-Infrared Illumination. Near-infrared illumination of the S_2-multiline state below 77 K induces a spin state transition, from spin 1/2 to spin 5/2. In plant PSII, the spin 5/2 state is characterized by signals at $g = 6$ and $g = 10$ while in *S. elongatus*, the spin 5/2 state is characterized by signals at $g = 5$ and $g = 9$ (*28*, *29*). In PSII cores from His-tagged *S. elongatus* essentially identical $g = 5$ and $g = 9$ signals were found upon IR illumination of the S_2-multiline state (result not shown).

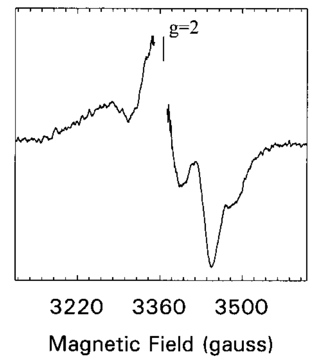

FIGURE 7: The split signal induced by IR light in S_3. Spectrum light-induced by an illumination at 820 nm, at 50 K, of His-tagged PSII cores from *S. elongatus* in the S_3-state. Instrument settings: standard cavity; temperature, 4.2 K; modulation amplitude, 2.8 G; microwave power, 20 mW; microwave frequency, 9.4 GHz; modulation frequency, 100 kHz. The central part of the spectra corresponding to the Tyr_D region was deleted.

Recently, it has been shown that near-infrared illumination of plant PSII in the S_3-state induced new EPR signals as well as some changes in the S_3-signals (*40*). Results from such an experiment using PSII cores from His-tagged *S. elongatus* are reported in Figure 6.

Spectra in panel A and B were recorded by using either perpendicular or parallel polarization EPR, respectively. PSII were trapped in the S_3-state (spectra a) by a protocol identical to that described in Figure 2, i.e., after two flashes. Spectra b were recorded after a subsequent illumination with a 820-nm light at 50 K. In panel A, spectrum c corresponds to the difference spectrum, spectrum b-minus-spectrum a, magnified 10 times.

In the perpendicular mode (panel A), near-infrared illumination produced a complex signal. The most intense feature is centered at $g = 2$ with a peak to trough equal to 176 G. In addition, signals at lower field and higher field (magnified in spectrum c) are also induced. Spectrum c exhibits a feature which peaks at $g = 5.20$ (turning point at $g = 4.35$) and a smaller peak at $g = 1.51$. The weak broad signal at around $g = 9$ corresponds to the $S = 5/2$ state induced by the illumination at 820 nm in the fraction of the centers remaining in the S_2-multiline state after illumination by two flashes (*29*). The 176-G-wide signal at $g = 2$ in PSII from *S. elongatus* is still detectable at 1.8 K, and the relative amplitude of the $g = 2$ and $g = 5.20$ signals remains almost constant between 1.8 and 10 K (results not shown).

In the parallel mode (panel B), the effect of near-infrared illumination is to shift the S_3-signal at $g = 14$ to a lower g-value ($g = 12$).

Figure 7 shows the 176-G-wide signal induced by near-infrared illumination using a low modulation amplitude and a small gain. Because the microwave relaxation properties of $Tyr_D^\bullet$ were slightly modified in the presence of the infrared-induced states (not shown), the recording of the central part of the spectrum was not possible.

In ammonia-treated plant PSII, it was found that the modified S_2-multiline state loses its susceptibility to near-

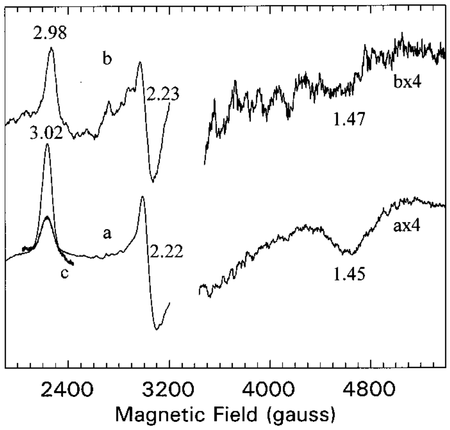

FIGURE 8: Isolated and membrane-bound Cytc_{550}. CW-EPR spectra of dark-adapted His-tagged PSII cores isolated from *S. elongatus* (spectrum a), of isolated Cytc_{550} (spectrum b) and of $CaCl_2$-washed PSII cores (spectrum c). Other instrument settings: standard cavity; temperature, 20 K; modulation amplitude, 32 G; microwave power, 2 mW; microwave frequency, 9.4 GHz; modulation frequency, 100 kHz. The right part of the spectra has been magnified 4 times.

infrared light. Here, a similar inhibition by ammonia of the infrared-induced spin-state transition in the Mn_4-cluster was found in PSII cores from His-tagged *S. elongatus* (not shown).

Isolated and Membrane-Bound Cytc$_{550}$. In Figure 8, the Cytc_{550} purified from isolated His-tagged PSII cores from *S. elongatus* (spectrum b) is compared to the spectrum recorded in intact PSII cores (spectrum a). Spectrum c was recorded on $CaCl_2$-washed PSII. The amplitude of spectrum c was scaled to that of spectrum a using the EPR signal of $Tyr_D^{\bullet}$ as a spin standard to estimate the PSII cores concentration.

In principle, the spectrum a could contain both the Cytb_{559} signal and the Cytc_{550} signal. However, in intact PSII, Cytb_{559} is expected to be in its high potential form, therefore reduced and thus EPR-silent, while Cytc_{550} is expected to be oxidized and thus detectable by EPR. $CaCl_2$ washing of *S. elongatus* results in the removal of Cytc_{550} from the majority of centers (*48*). The EPR signal from the heme is indeed much smaller after this treatment. However, in plant PSII, salt-washing treatments that remove the extrinsic polypeptides also convert Cytb_{559} to a low-potential form leading to its oxidation at ambient potential (*65*). If this occurs in *S. elongatus* then oxidized Cytb_{559} may well contribute significantly to this spectrum.

The isolated Cytc_{550} (Figure 8, spectrum b) does not exhibit very different *g*-values from those measured in situ (spectrum a). This contrasts with the situation observed with Cytb_{559} for which the *g* values measured in vitro are significantly different from those measured in situ (e.g., refs *66* and *67*). The *g*-values found here in *S. elongatus* for both the isolated and membrane-bound Cytc_{550} are similar to those found in *Synechococcus* 7942 (*68*) and in *Microcystis aeruginosa* (*69*).

Orientation of Cytc$_{550}$. Figure 9 shows a study of the heme signals in an oriented sample. His-tagged PSII cores from *S. elongatus* were oriented on Mylar sheet, and spectra were recorded for different angles between the plane of the Mylar sheet and the magnetic field direction. The nature of the sample orientation was verified by studying the EPR signal from Tyr_D (not shown), and the data were qualitatively similar to those reported earlier in oriented PSII membranes, although the degree of orientation was less good. It can be concluded that, as expected, the detergent-depleted PSII cores associate in sheetlike structures that reflect the membrane structure.

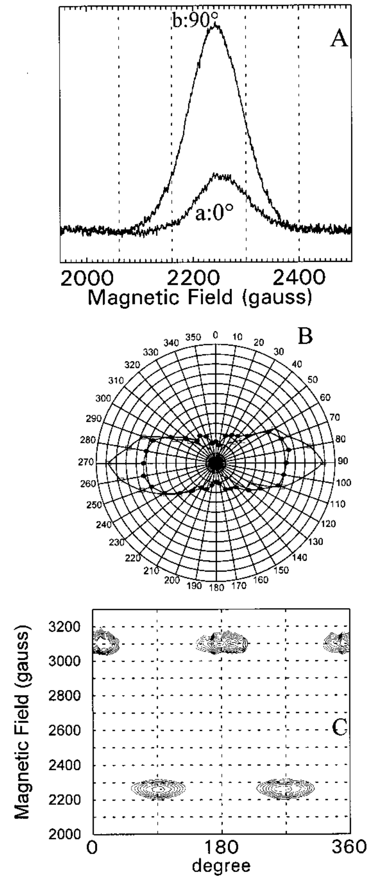

FIGURE 9: Orientation of Cytc_{550}. Panel A: g_z signal of cytochrome(s) detected in His-tagged PSII cores isolated from *S. elongatus*. The angle is that defined by the normal to the Mylar sheet and the direction of the magnetic field. Other instrument settings: standard cavity; temperature, 15 K; modulation amplitude, 32 G; microwave power, 2 mW; microwave frequency, 9.4 GHz; modulation frequency, 100 kHz. Panel B: area from 2060 to 2160 G (squares) and from 2300 to 2400 G (circles) of the g_z signal (see vertical dashed lines in panel A). Same instrument settings as in panel A. Panel C: contour plot of the g_z and g_y signals detected in His-tagged PSII cores isolated from *S. elongatus*. Same instrument settings as in panel A.

Panel A in Figure 9 shows the signal in the g_z magnetic field region for two angles (0 and 90°) between the normal to the Mylar plane and the magnetic field direction. The g_z and g_y signals were measured by 10° steps from 0 to 360° (panels B and C, Figure 9). The data show a clear orientation dependence in which the g_z signal was maximum when the Mylar plane was parallel to magnetic field direction, while the g_y signal was maximal when the Mylar plane was perpendicular to the magnetic field. This indicates that the heme plane is oriented perpendicular to the Mylar and thus the membrane plane.

After the drying period, it is possible that a proportion of Cytb_{559} converts to its low potential form and thus becomes oxidized. However, given the apparent dominance of the Cytc_{550} signal, due to its redox properties and perhaps its greater stoichiometry, and given the unusual stability of the protein complex (and hence the likelihood that Cytb_{559} remains in its high potential form), the expected contribution from Cytb_{559} may be small. Even so, since both cytochromes have similar spectra, it is possible that the spectra represent a superimposition of the signals from the heme of Cytb_{559} and from Cytc_{550}. If the actual position of the g_z lines are slightly different in terms of their field position and if the orientations of the two hemes are different, it may be possible to differentiate between their contributions in the orientation experiment. The following procedure was performed with this aim. Spectra in the region of the g_z signals were recorded for all the orientations of the Mylar sheet in the magnetic field. Then, the area of the signal from 2060 to 2160 G (squares in panel B, Figure 9) and that of the signal from 2300 to 2400 G (circles in panel B, Figure 9) were plotted separately versus the angle between the normal to the Mylar and the magnetic field direction. Both data sets show that the g_z signal was maximum when the plane of the PSII cores was parallel to magnetic field direction. This is the same as the orientation of Cytb_{559} as measured earlier in plant PSII. Since the Cytc_{550} seems to be the dominant signal in intact membranes, it seems reasonable to conclude that the orientation of its ring plane is also close to perpendicular to the membrane. From the present study, we are unable to determine if Cytb_{559} contributes to the orientation data.

DISCUSSION

In the present work, we have surveyed several of the EPR properties of PSII from *S. elongatus* using reaction center cores isolated from a His-tagged CP43 strain. The results in Figures 1 show that both the S_2-mutiline and S_0-multiline signals are virtually identical to those detected in PSII cores isolated from the non-His-tagged strain (*29*, *30*). In addition, the EPR spectrum of the spin 5/2 S_2-state induced by infrared illumination is almost identical to that found previously (*29*) (not shown). It can thus be concluded that the His-tag does not induce structural perturbations of the Mn_4.

It has recently been reported that in His-tagged *Synechocystis* 6803 a $g = 4.1$ signal could be generated under conditions used to generate the S_2-multiline signal (*45*). Apart from this brief report, the $g = 4$ signal had not been reported in PSII from cyanobacteria raising the question whether the His-tag itself may be responsible for perturbing the Mn cluster. As stated above, in the present study the His-tag had no evident effect on the Mn cluster as judged by the EPR spectra. In an earlier study (*29*) of PSII in *S elongatus* in which the question of the missing $g = 4$ signal was addressed, it was suggested that the state exists but it is unstable relative to the state giving rise to the second form of the spin = 5/2 state of S_2. In the present study, the $g = 4$ state was observed in PSII from *S. elongatus* when treated with ammonia or acetate, i.e., under the same conditions as in plant PSII in which these treatments were shown to induce a type of (partial) chloride depletion. This fits with the idea that the structural conformation that gives rise to the "$g = 4$ state" can be stabilized to different degrees by appropriate biochemical conditions.

In plant PSII, EPR signals in the S_3-state were first detected by Matsukawa et al. (*39*). The S_3-state exhibited signals in both perpendicular (at $g = 6.7$) and parallel (at $g = 12$ and $g = 8$) polarization modes. These signals were interpreted as originating from different transitions in the same spin = 1 state or from a spin = 2 state resulting from the interaction between an organic radical (spin = 1/2) and the Mn_4-cluster with a spin state equal to 3/2 (*39*). These results were confirmed very recently under conditions in which the S_3-state was formed with a higher yield (*40*) (i.e., in 50−60% of the reaction centers). In this work (*40*), the S_3-signal in the perpendicular mode was seen at $g = 10$. The authors favored the magnetic interaction between a radical and the Mn cluster to explain the spectra (*40*). In both of these reports (*39*, *40*), it was shown that the presence of certain organic solvents diminishes or eliminates the S_3 signals. It seems that the organic solvents (particularly alcohols) used for dissolving artificial electron acceptors may have rendered the S_3 signals undetectable in previous studies. In *S. elongatus*, the presence of the intrinsic secondary electron acceptor quinone, Q_B, makes the addition of PPBQ unnecessary for the first few turnovers. In Figure 2, it can be estimated that illumination of PSII, presynchronized in the S_1-state by two saturating flashes, formed the S_3-state in about 75% of the reaction centers. Under these conditions, signals are detected both in perpendicular (broad signal at $g = 10$) and parallel (at $g = 14$ and $g = 8$) polarization modes. These g values differ slightly from those observed in the S_3-state in plant PSII (*39*, *40*).

Biochemical modifications of the oxygen evolving enzyme in plant PSII, such as the substitution of Ca^{2+} for Sr^{2+} or ammonia binding, result in modified forms of the S_2-signals (*11*, *12*, *25*, *28*). In this work, effects of such treatments have been investigated in His-tagged PSII cores from *S. elongatus*. This is of relevance since there are several reports in the literature that indicate that the behavior of PSII in cyanobacteria and in particular the species used in the present strain seems to be different with regard to the influence of Ca^{2+} and Cl^- (e.g., ref *70*).

In the ammonia-treated sample (Figure 3), illumination at 190 K resulted in a normal S_2-multiline signal. This behavior is similar to that observed in plant PSII (*11*, *25*, *28*) and as in plant PSII, in *S. elongatus* the modification of the S_2-multiline signal occurred after the sample was warmed to a temperature that allows ammonia to bind to its site. The modified S_2-multiline signal observed in Figure 3 (spectrum b) is essentially identical to that observed in ammonia-treated plant PSII (*13*, *28*, *57*). Spectrum a in Figure 3 also shows that, in a fraction of the centers, a signal at $g = 4.25$ is light-induced at 190 K. The present observation demonstrates that the structural conformation of the Mn_4-cluster at the origin of the $g = 4$ signal can occur in *S. elongatus*. In ammonia-treated plant PSII, the presence of the $g = 4.25$ signal was attributed to the binding of NH_3 in a different site from that giving rise to the modified multiline signal but one that is competitive with Cl^- (*25*), and it seems likely that a similar situation exists in *S. elongatus*.

Ammonia modifies the EPR properties of the S_2-state (see above). However, the structural change at the origin of this effect does not result in inhibition of oxygen evolution (*58*). This was interpreted by a model in which ammonia is quickly replaced by the normal substrate (i.e., a water molecule) in the S_4-state. Inhibition of oxygen evolution only occurred after a dark period in the S_3-state long enough to allow a second ammonia to bind to a second site (*58*, *71*). To test further this model in His-tagged *S. elongatus*, the effect of ammonia on the EPR properties of the S_3-state was investigated (Figure 4). Signals both in parallel and perpendicular polarization modes were detected. These signals are similar but not identical to those measured in the untreated sample. Although the biochemical conditions are different in the two samples, it is tempting to attribute the observed differences to ammonia itself. Consequently, this would indicate that, as expected (*58*, *71*), ammonia is still in its site in the S_3-state.

Reconstitution of Ca^{2+}-depleted plant PSII by Sr^{2+} restores about 40% of the oxygen evolution activity (*12*, *72*). This decrease in the activity is probably due to a slow down of the S_2 to S_3 and S_3 to S_0 transitions (*73*). In plant PSII, the Sr^{2+}-reconstituted preparations exhibit a modified multiline signal and an intense $g = 4.25$ signal in the S_2-state (*12*). Spectrum c in Figure 3 shows that a modified S_2-multiline signal is also formed in a fraction of the Sr^{2+}-reconstituted His-tagged *S. elongatus*; however, a $g = 4$ signal is not observed. Instead a signal that peaks at $g = 5.20$ is formed. This is tentatively attributed to a spin 5/2 form of the Mn cluster that differs slightly from the state that gives rise to the $g = 4$ signal.

Acetate addition to *Synechococcus* has been shown to inhibit the reduction of P_{680}^+ under repetitive flash illumination at room temperature (*74*). In plants and/or *Synechocystis*, acetate-treated PSII are inhibited at the $S_2Tyr_Z^\bullet$ step upon illumination at 0 °C similarly to the situation in observed in Ca^{2+}-depleted and Cl^--depleted PSII (*13*, *61*, *62*, *64*, *73*, *75*). In fact, it has been shown that acetate treatment results in a chloride depletion (*76*) in a competitive manner (*77*). The $S_2Tyr_Z^\bullet$ state is characterized by a split EPR signal arising from the magnetic interaction between a radical (*13*), identified as a tyrosyl radical (*64*), and the Mn_4-cluster. The shape of the $S_2Tyr_Z^\bullet$ depends on the biochemical conditions. In plant PSII, the differences between the split signal in acetate-treated PSII and Ca^{2+}-depleted/EGTA-treated PSII have been simulated assuming that the coupling between the Mn-cluster and the radical is ferromagnetic in the former and antiferromagnetic in the latter (*78*). In cyanobacteria, a split $S_2Tyr_Z^\bullet$ signal has already been observed in EGTA-treated PSII from *Synechocystis* (*60*) and in a D1-H332E (*79*) and D1-glu189 (*80*) mutants of *Synechocystis* 6803. Figure 5 shows the effect of acetate on *S. elongatus*.

The structure of the $S_2Tyr_Z^\bullet$ signal in acetate-treated PSII cores from S. *elongatus* (and to a lesser extent the width, 232 G, peak to trough) differs slightly from the corresponding values in plant PSII (240 G, peak to trough). This means that the magnetic interaction between the metal and the radical is similar but not identical. This could be due to a change either in the distance or the angle between the magnetic axes of the radical and of the Mn_4-cluster but quantification of these differences is premature.

Recently, it has been shown that the S_3-state in plant PSII is sensitive to near-infrared light (*40*). This was confirmed in the present work in which we found that illumination at 820 nm in the S_3-state of His-tagged PSII from *S. elongatus* induced new EPR signals in both perpendicular and parallel modes (Figure 6). In the perpendicular mode, a 176-G-wide split signal at $g = 2$ is formed (seen with a better resolution in Figure 7), together with a broad positive signal (which peaks at $g = 5.2$) and a smaller negative signal (which peaks at $g = 1.51$). These infrared-induced signals resemble those induced in plant PSII (*40*), but the $g = 1.51$ seen here was not detected in plant PSII (*40*) and the split $g = 4$ signal seen in ref *40* was not detected here.

In the S_3-state modified by ammonia, infrared irradiation was found to have no effect. This indicates that the modifications induced by ammonia in the structure of the oxygen evolving system and making infrared light ineffective in S_2 are also conserved in the S_3-state in PSII cores from *S. elongatus*.

The observation that the Mn_4-cluster is IR-photoactive in both S_2 and S_3 (at least in a proportion of the centers) can be taken as an indication that the structure and valence of the Mn (or at least the photoactive motif) are similar in both of these states. This then supports recent models in which a ligand-centered oxidation seems to be preferred to a metal-centered oxidation in the S_2 to S_3 transition (*8*). The 176-G-wide split signal observed in this work and earlier (*40*) is reminiscent of the $S_2Tyr_Z^\bullet$ split signal. This led Ioannidis and Petrouleas (*40*) to propose that, upon absorption of infrared light at 50 K, the Mn_4 complex becomes so oxidizing that it can abstract an electron from an organic molecule (Tyr_Z for example). Alternatively, the organic radical could be that invoked in models that favor the ligand-centered oxidation in the S_2 to S_3 transition (*8*). If so, the infrared light would induce a structural change making the magnetic coupling between this radical and the Mn_4-cluster smaller and hence making the S_3-state detectable by EPR.

Detection of the 176-G-wide split signal at 1.8 K in the infrared illuminated S_3-state suggests that the radical would be magnetically coupled to a faster relaxer than the spin 1/2 S_2-state. The $g = 5.20$ and $g = 1.51$ signals could correspond to signals from this fast relaxer state. By comparison, in acetate-treated plant PSII, the split signal arises from a slower relaxing species: the half-saturation of the magnetically coupled radical in the $S_2Tyr_Z^\bullet$ state occurred at a slightly lower power than the spin 1/2 S_2-manganese signal (*81*) (see also ref *82* for the relaxation properties of the radical and of the manganese signal in the $S_2Tyr_Z^\bullet$ state in EGTA-treated PSII). As a consequence, the $S_2Tyr_Z^\bullet$ split signal is no longer detectable at 4 K.

One difficulty in making firmer assignments at present is that the changes seen seem to occur in only a fraction of centers, and thus the samples clearly show heterogeneity. For example, the signal at $g = 10$ in the perpendicular mode seems unaffected by the infrared illumination. This can be explained if the infrared light affects only a proportion of the PSII centers and that those centers are different from those giving rise to the $g = 10$ signal. A similar kind of heterogeneity has already been observed in the S_2-state, where all the reaction centers are not equally susceptible to infrared light (*83*). Whatever the model drawn, the complexity of the data makes quantification difficult.

The signals induced by infrared illumination in the S_3-states seen here and earlier (*40*) resemble those detected after a complex protocol including different illumination periods at different temperatures (*84*). This can be explained if we assume that (i) the protocol used in ref *84* (i.e., freezing under illumination) resulted in formation of the S_3-state in a small fraction of the PSII reaction centers and (ii) the subsequent illumination at 30 K, after which these signals were observed, contained infrared light. Both assumptions seem reasonable.

His-tagged PSII cores from *S. elongatus* were oriented on Mylar sheets to study the orientation of the heme of Cytc_{550}.

One difficulty in the interpretation of the data is the potential superimposition of the Cytb_{559} spectrum on that of the Cytc_{550} spectrum. Despite this problem, data in Figure 9 show that the heme plane of Cytc_{550} is perpendicular to the membrane plane and if Cytb_{559} is present it is oriented the same way as expected from earlier studies (*55*).

CONCLUSION

The present work shows that *S. elongatus* PSII cores are well-suited to EPR studies. The results extend the comparisons begun between cyanobacterial PSII and plant PSII, and so far the differences found, although spectroscopically significant, probably represent no fundamental difference in structure. The orientation of the Cytc_{550} heme plane is a further piece of structural information to add to the model constructed from spectroscopic studies. The presence of functional Q_B allows several turnovers (required for the efficient formation of S_3) without the necessity to add artificial lipophilic acceptors. The clearly defined S_3 signals reported here for the first time in cyanobacteria confirm the recent report from plant PSII and show that these signals can be used to monitor modifications of PSII, as demonstrated here by the modifications induced in NH_3-treated PSII. The present work then will act as a basis for future spectroscopic and molecular enzymological work.

ACKNOWLEDGMENT

N. Ioannidis and V. Petrouleas are acknowledged for communication of their manuscript prior to publication. H. Bottin and S. Un are acknowledged for discussions. G. Moal and B. Lagoutte are acknowledged for their help in HPLC purification.

REFERENCES

1. Debus R. J. (2000) in *Metal Ions in Biological Systems* (Sigel, H., and Sigel, A., Eds.) Vol. 37, pp 657−711, Marcel Dekker, Inc., New York.
2. Nield, J., Orlova, E. V., Morris, E. P., Gowen, B., van Heel, M., and Barber, J. (2000) *Nature Struct. Biol. 7*, 44−47.
3. Britt, R. D. (1996) in *Oxygenic Photosynthesis: The Light Reactions* (Ort, D. R., Yocum, C. F., Eds.) pp 137−164, Kluwer Academeic Publishers, Dordrecht.
4. Debus, R. J. (1992) *Biochim. Biophys. Acta 1102*, 269−352.
5. Tommos, C., and Babcock, G. T. (1998) *Acc. Chem. Res. 31*, 18−25.
6. Hoganson, C. W., and Babcock, G. T. (2000) in *Metals in Biological Systems* (Sigel, H., and Sigel, A., Eds.) Vol. 37, pp 613−656, Marcel Dekker, Inc., New York.
7. Yachandra, V. K., Sauer, K., and Klein, M. P. (1996) *Chem. Rev. 96*, 2927−2950.
8. Liang, W., Roelofs, T. A., Cinco, R. L., Rompel, A., Latimer, M. J., Yu, W. A., Sauer, K., Klein, M. P., and Yachandra, V. (2000) *J. Am. Chem. Soc. 122*, 3399−3412.
9. Dismukes, G. C., and Siderer, Y. (1981) *Proc. Natl. Acad. Sci. U.S.A. 78*, 274−278.
10. Zheng, M., and Dismukes, G. C. (1996) *Inorg. Chem. 35*, 3307−3319.
11. Beck, W. F., and Brudvig, G. W. (1986) *Biochemistry 25*, 6479−6486.
12. Boussac, A., and Rutherford, A. W. (1988) *Biochemistry 27*, 3476−3483.
13. Boussac, A., Zimmermann, J.-L., and Rutherford A. W. (1989) *Biochemistry 28*, 8984−8989.
14. Britt, R. D., Zimmermann, J.-L., Sauer, K., and Klein, M. P. (1989) *J. Am. Chem. Soc. 111*, 3522−3532.
15. Zimmermann, J.-L., and Rutherford, A. W. (1984) *Biochim. Biophys. Acta 767*, 160−167.
16. Zimmermann, J.-L., and Rutherford, A. W. (1986) *Biochemistry 25*, 4609−4615.
17. Casey, J. L., and Sauer, K., (1984) *Biochim. Biophys. Acta 767*, 21−28.
18. de Paula, J. C., Innes, J. B., and Brudvig, G. W. (1985) *Biochemistry 24*, 8114−8120.
19. Boussac, A., Girerd, J.-J., and Rutherford, A. W. (1996) *Biochemistry 35*, 6984−6989.
20. Boussac, A., and Rutherford, A. W. (2000) *Biochim. Biophys. Acta 1457*, 145−156.
21. van Vliet, P., and Rutherford, A. W. (1996) *Biochemistry 35*, 1829−1839.
22. Lindberg, K., and Andréasson, L.-E. (1996) *Biochemistry 35*, 14259−14267.
23. Ono, T.-A., Nakayama, H., Gleiter, H., Inoue, Y., and Kawamori, A. (1987) *Arch. Biochem. Biophys. 256*, 618−624.
24. van Vliet, P., (1996) Thesis, Landbouwuniversiteit Wageningen.
25. Beck, W. F., dePaula, J. C., and Brudvig, G. W. (1986) *J. Am. Chem. Soc. 108*, 4018−4022.
26. Horner, O., Rivière, E., Blondin, G., Un, S., Rutherford, A. W., Girerd, J.-J., and Boussac, A. (1998) *J. Am. Chem. Soc. 120*, 7924−7928.
27. Haddy, A., Dunham, W. R., Sands, R. H., and Aasa, R. (1992) *Biochim. Biophys. Acta 1099*, 25−34.
28. Boussac, A., Un, S., Horner, O., and Rutherford, A. W. (1998) *Biochemistry 37*, 4001−4007.
29. Boussac, A., Kuhl, H., Un, S., Rögner, M., and Rutherford, A. W. (1998) *Biochemistry 37*, 8995−9000.
30. Boussac, A., Kuhl, H., Ghibaudi, E., Rögner M., and Rutherford, A. W. (1999) *Biochemistry 38*, 11942−11948.
31. Messinger, J., Nugent, J. H. A., and Evans, M. C. W. (1997) *Biochemistry 36*, 11055−11060.
32. Messinger, J., Robblee, J. H., Yu, W. O., Sauer, K., Yachandra, V. K., and Klein, M. P. (1997) *J. Am. Chem. Soc. 119*, 11349−11350.
33. Åhrling, K. A., Peterson, S., and Styring, S. (1997) *Biochemistry 36*, 13148−13152.
34. Åhrling, K. A., Peterson, S., and Styring, S. (1998) *Biochemistry 37*, 8115−8120.
35. Dexheimer, S. L., and Klein, M. P. (1992) *J. Am. Chem. Soc. 114*, 2821−2826.
36. Yamauchi, T., Mino, H., Matsukawa, T., Kawamori, A., and Ono, T.-A. (1997) *Biochemistry 36*, 7520−7526.
37. Campbell, K. A., Peloquin, J. M., Pham, D. P., Debus, R. C., and Britt, R. D. (1998) *J. Am. Chem. Soc. 120*, 447−448.
38. Campbell, K. A., Gregor, W., Pham, D. P., Peloquin, J. M., Debus, R. C., and Britt, R. D. (1998) *Biochemistry 37*, 5039−5049.
39. Matsukawa, T., Mino, H., Yoneda, D., and Kawamori, A. (1999) *Biochemistry 38*, 4072−4077.
40. Ioannidis, N., and Petrouleas, V., (2000) *Biochemistry 39*, 5246−5254.
41. Nield, J., Kruse, O., Ruprecht, J., da Fonseca, P., Büchel, C., and Barber, J. (2000) *J. Biol. Chem. 275*, 27940−27946.
42. Zouni, A., Jordan, R., Schlodder, E., Fromme, P., and Witt, H. T. (2000) *Biochim. Biophys. Acta 1457*, 103−105.
43. Kuhl, H., Kruip, J., Seidler, A., Krieger-Liszkay, A., Bünker, M., Bald, D., Scheidig, J., and Rögner, M. (2000) *J. Biol. Chem. 275*, 20652−20659.
44. Sugiura, M., Inoue, Y., and Minagawa, J. (1998) *FEBS Lett. 426*, 140−144.
45. Reifler, M. J., Chisholm, D. A., Wang, J., Diner, B. A., and Brudvig, G. W. (1998) in *Photosynthesis: Mechanism and Effects* (Garab, G., Ed.) Vol II, pp 1189−1192, Kluwer Academic Publisher, The Netherlands.
46. Bricker, T. M., Morvant, J., Masri, N., Sutton, H. M., and Frankel, L. K. (1998) *Biochim. Biophys. Acta 1409*, 50−57.
47. Campbell, K. A., Ann Force, D., Nixon, P. J., Dole, F., Diner, B. A., and Britt, R. D. (2000) *J. Am. Chem. Soc. 122*, 3754−3761.

48. Sugiura. M., and Inoue, Y. (1999) *Plant Cell Physiol. 40*, 1219−1231.
49. Kuhl, H., Rögner, M., van Breemen, J. F. L., and Boekema, E. J. (1999) *Eur. J. Biochem. 266*, 453−459.
50. Shen, J.-R., Ikeuchi, M., and Inoue, Y. (1992) *FEBS Lett. 301*, 145−149.
51. Shen, J.-R., and Inoue, Y. (1993) *J. Biol. Chem.* 268, 20408−20413.
52. Nishiyama, Y., Hayashi, H., Watanabe, T., and Murata, N. (1994) *Plant Physiol. 105*, 1313−1319.
53. Shen, J.-R., Burnap, R. L., and Inoue, Y. (1995) in *Photosynthesis: From Light to Biosphere* (Mathis, P., Ed.) Vol. II, pp 559−562, Kluwer Academic Publisher, The Netherlands.
54. Kuwabara, T., Miyao, M., Murata, T., and Murata, N. (1985) *Biochim. Biophys. Acta 806*, 283−289.
55. Rutherford, A. W. (1985) *Biochim. Biophys Acta 807*, 189−201.
56. Diner, B. A., Petrouleas, V., and Wendoloski, J. J. (1991) *Physiologia Plantarum 81*, 423−436.
57. Koike, H., and Inoue, Y., (1985) *Biochim. Biophys. Acta 807*, 64−73.
58. Boussac, A., Rutherford, A. W., and Styring, S. (1990) *Biochemistry 29*, 24−32.
59. Sandusky, P. O., and Yocum, C. F., (1983) *FEBS Lett. 162*, 339−343.
60. Kirilovsky, D. L., Boussac, A. G. P., van Mieghem, F. J. E., Ducruet, J.-M. R. C., Sétif, P. R., Yu, J., Vermaas, W. F. J., and Rutherford, A. W. (1992) *Biochemistry 31*, 2099−2107.
61. MacLachlan, D. J., and Nugent, J. H. A. (1993) *Biochemistry 32*, 9772−9780.
62. Szalai, V. A., and Brudvig, G. W. (1996) *Biochemistry 35*, 15080−15087.
63. Vermaas, W. F. J., and Rutherford, A. W. (1984) *FEBS Lett. 175*, 243−248.
64. Tang, X. S., Randall, D. W., Force, D. A., Diner, B. A., and Britt, R. D. (1996) *J. Am. Chem. Soc. 118*, 7638−7639.
65. Stewart, D. H., and Brudvig, G. W. (1998) *Biochim. Biophys. Acta 1367*, 63−87.
66. Babcock, G. T., Widger, W. R., Cramer, W. A., Oertling, W. A., and Metz, J. G., (1985) *Biochemistry 24*, 3638−3645.
67. Berthomieu, C., Boussac, A., Mäntele, W., Breton, J., and Nabedryk, E. (1992) *Biochemistry 31*, 11460−11471.
68. Hoganson, C. W., Lagenfelt, G., and Andréasson, L.-E. (1990) *Biochim. Biophys. Acta 1016*, 203−206.
69. Kang, C., Chitnis, P. R., Smith, S., and Krogmann, D. W. (1994) *FEBS Lett. 344*, 5−9.
70. Pauly, S., Schlodder, E., and Witt, H. T. (1992) *Biochim. Biophys. Acta 1099*, 203−210.
71. Velthuys, B. R. (1975) Thesis, University of Leiden. The Netherlands.
72. Ghanotakis, D. F., Babcock, G. T., and Yocum, C. F. (1984) *FEBS Lett. 167*, 120−130.
73. Boussac, A., Sétif, P., and Rutherford, A. W. (1992) *Biochemistry 31*, 1224−1234.
74. Bok, C. H., Gerken, S., Stehlik, D., and Witt, H. T. (1988) *FEBS Lett. 227*, 141−146.
75. Boussac, A., Zimmermann, J.-L., Rutherford, A. W., and Lavergne, J. (1990) *Nature 347*, 303−306.
76. Sinclair, J. (1984) *Biochim. Biophys. Acta 764*, 247−252.
77. Szalai, V. A., and Brudvig, G. W. (1999) *Biochemistry 38*, 15080−15087.
78. Dorlet, P., Boussac, A., Rutherford, A. W., and Un, S. (1999) *J. Phys. Chem. B. 103*, 10945−10954.
79. Debus, R. J., Campbell, K. A., Peloquin, J. M., Pham, D. P., and Britt, R. D. (2000) *Biochemistry 39*, 470−478.
80. Debus, R. J., Campbell, K. A., Pham, D. P., Hays, A.-M. A., and Britt, R. D. (2000) *Biochemistry 39*, 6275−6287.
81. Szalai, V. A., Kühne, H., Lakshmi, K. V., and Brudvig, G. W. (1998) *Biochemistry 37*, 13594−13603.
82. Boussac, A., Zimmermann, J.-L., and Rutherford, A. W. (1990) in *Current Research in Photosynthesis* (M. Baltscheffsky, Ed.), Vol. I, pp 713−716, Kluwer, Dordrecht.
83. Boussac, A. (1997) *J. Biol. Inorg. Chem. 2*, 580−585.
84. Nugent, J. H. A., Turconi, S., and Evans, M. C. W. (1997) *Biochemistry, 36*, 7086−7096.

BI001159R